ICFA 17th Adv. Beam Dynamics Workshop on Future Light Sources, Argonne, IL, April 6-9, 1999.

High Energy Electron Injection and Acceleration with Intense Short Pulse Lasers

Antonio C. Ting*
Plasma Physics Division
Naval Research Laboratory
Washington, DC 20375

Supported by DoE, Omega-P, Inc., and ONR

* Collaborators: C.I. Moore, T. Jones,[1] S. McNaught,[2] R. Burrris,[3] J. Qiu,[4] P. Sprangle, and B. Hafizi[1]

[1] Icarus Research, Inc., Bethesda, MD

[2] University of Rochester, Rochester, NY

[3] RSI Inc., Lanham, MD

[4] NRC/NRL post-doc

Outline

- Motivation
  - Laser driven accelerators -- LWFA
  - Needs external electron injection
- Laser driven electron injectors
- Laser Ionization and Ponderomotive Acceleration (LIPA)
  - Mechanism
  - Experiment
  - Simulations
- Conclusions

Laser Wakefield Accelerator

- A short intense laser pulse propagating through a plasma excites a plasma wave in the laser pulse's wake (a "wakefield" plasma wave) by the laser's ponderomotive force.

- Externally injected electrons can be accelerated to high energies by the large amplitude electric fields in the plasma

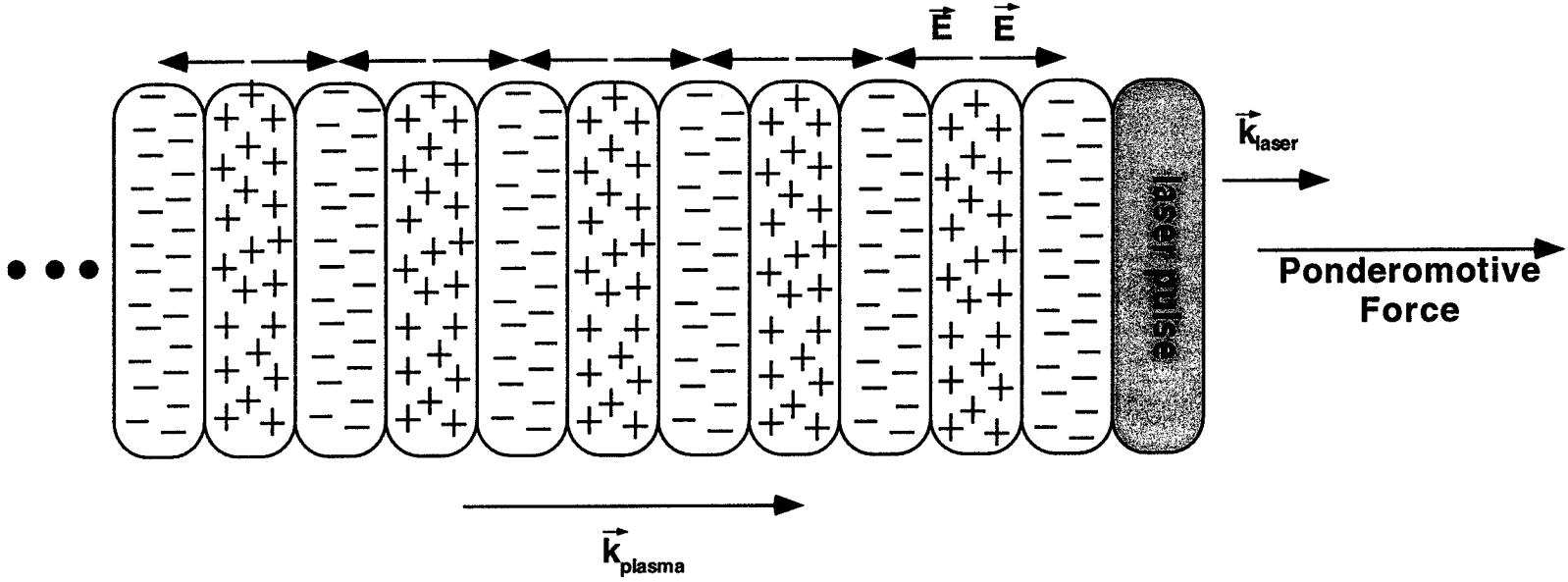

Recent results from the NRL SM-LWFA experiment

- Peak energy ~ 100 MeV
- Peak Acceleration field = 100-500 GV/m
- Wakefield Amplitude, $\Delta n/n_0 \approx 1$
- Laser Power 2.5 TW

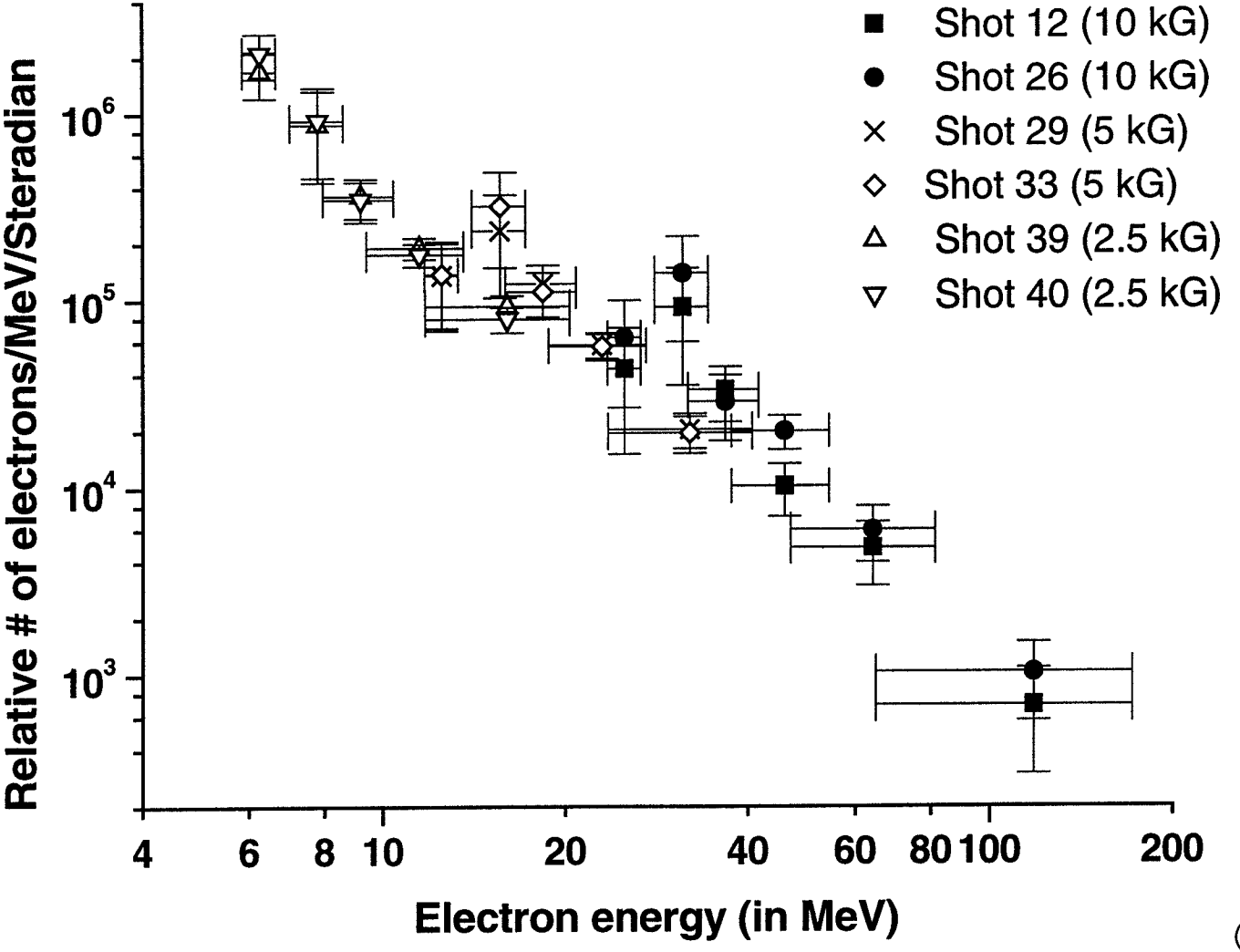

NRL

Comparison between SM-LWFA and LWFA

SM-LWFA

- Self-trapped electrons accelerated with large energy spread (~100%).
- Plasma period short (~20 fs), difficult to inject electrons.
- Extended acceleration distance from relativistic self-focusing (RSF).

LWFA

- Injected electrons could be accelerated with small energy spread .
- Longer plasma period (~100 fs), may inject electrons at desired acceleration phase.
- RSF is not applicable in LWFA due to low plasma density and short pulse.

NRL

Photo-cathode RF gun injection

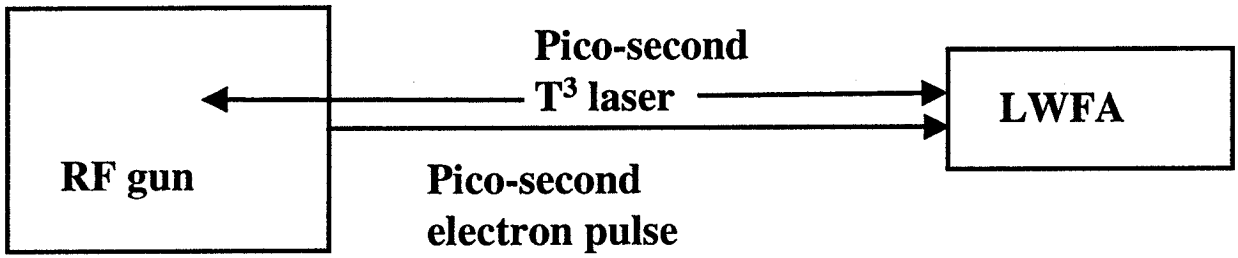

- Requires RF gun.
- Requires photo-cathode in RF gun.
- Requires synchronization between RF gun and laser.
- Requires electron beam optics.
- Electron pulses not short enough for precise phasing with wakefield.

Laser Driven Electron Injectors

- **LILAC (Laser Injection Laser Accelerator)[1]**
- **Colliding pulses[2]**
- **LIPA (Laser Ionization and Ponderomotive Acceleration)[3]**

[1] D. Umstadter et al., PRL, 76, 2073 (1996)

[2] E. Esarey et al., PRL, 79, 2682 (1997)

[3] C.I. Moore et al., PRL, 82, 1688 (1999)

Laser Injection Laser Accelerator (LILAC)

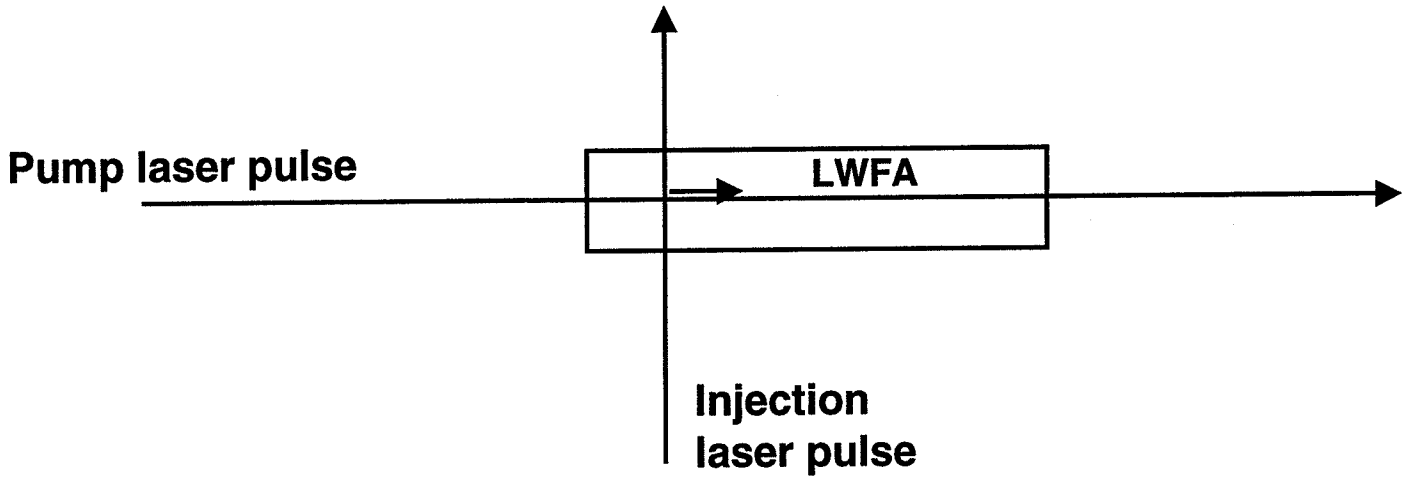

- Intense pump laser pulse excites wakefield in LWFA.

- Intense injection laser pulse perturb plasma electrons to be trapped by wakefield of LWFA.

- Temporal and spatial alignment of pump and injection laser pulses determines acceleration phase.

Colliding Pulse Injector

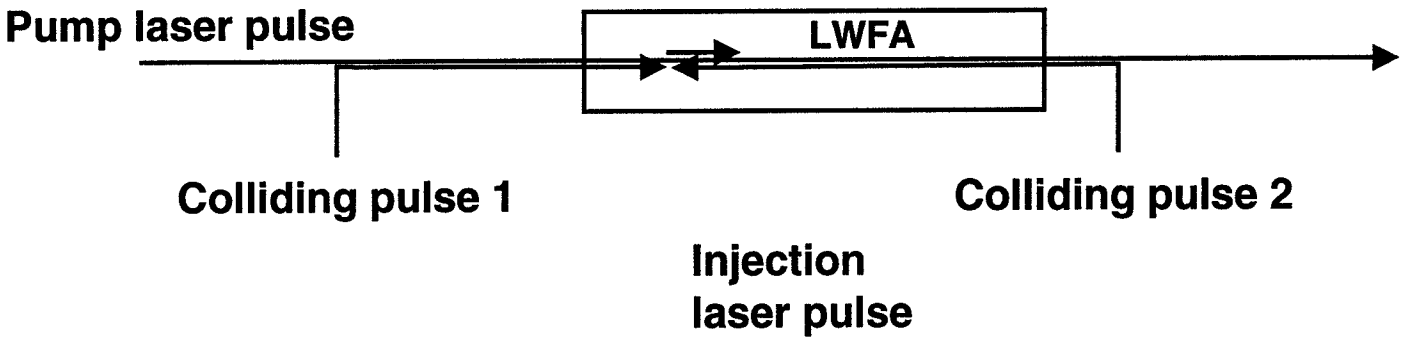

- Intense pump laser pulse excites wakefield in LWFA.
- Colliding pulses form low phase velocity beatwave to trap plasma electrons.
- Synchronization between pump and colliding pulse 1 determines acceleration phase.

Laser Ionization and Ponderomotive Acceleration (LIPA) Injection

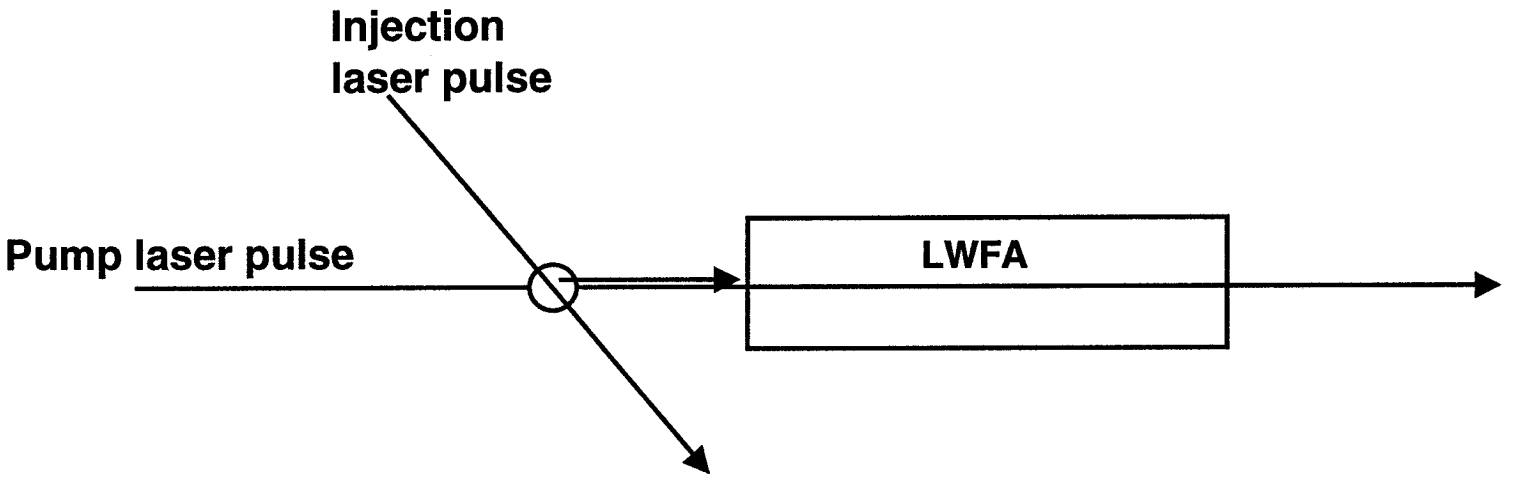

- Injection source is outside LWFA and will not interfere with wakefield.
- Injection energy can be tailored with choice of ionization of gas and selected with alignment angle.
- Electron pulse length much shorter than injection laser pulse length.
- Relative ease of laser alignment.

The laser ionization and ponderomotive acceleration (LIPA) of high charge state ions produces energetic electrons from a high intensity laser focus (E ~ 1 MeV @ 10^{19} W/cm^2)

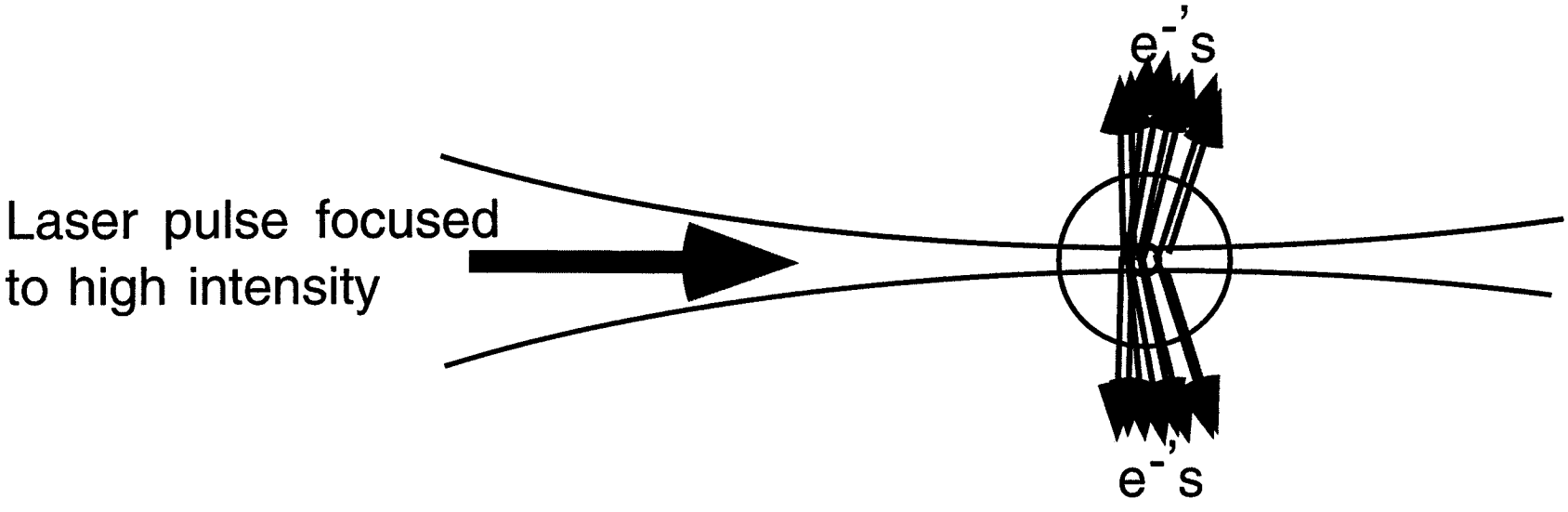

Tunneling ionization and its strong field limit (Barrier Suppression Ionization - BSI) describe high intensity ionization in a 1 μm field ($\gamma_{Keldysh} = \sqrt{E/2U_p} << 1$)

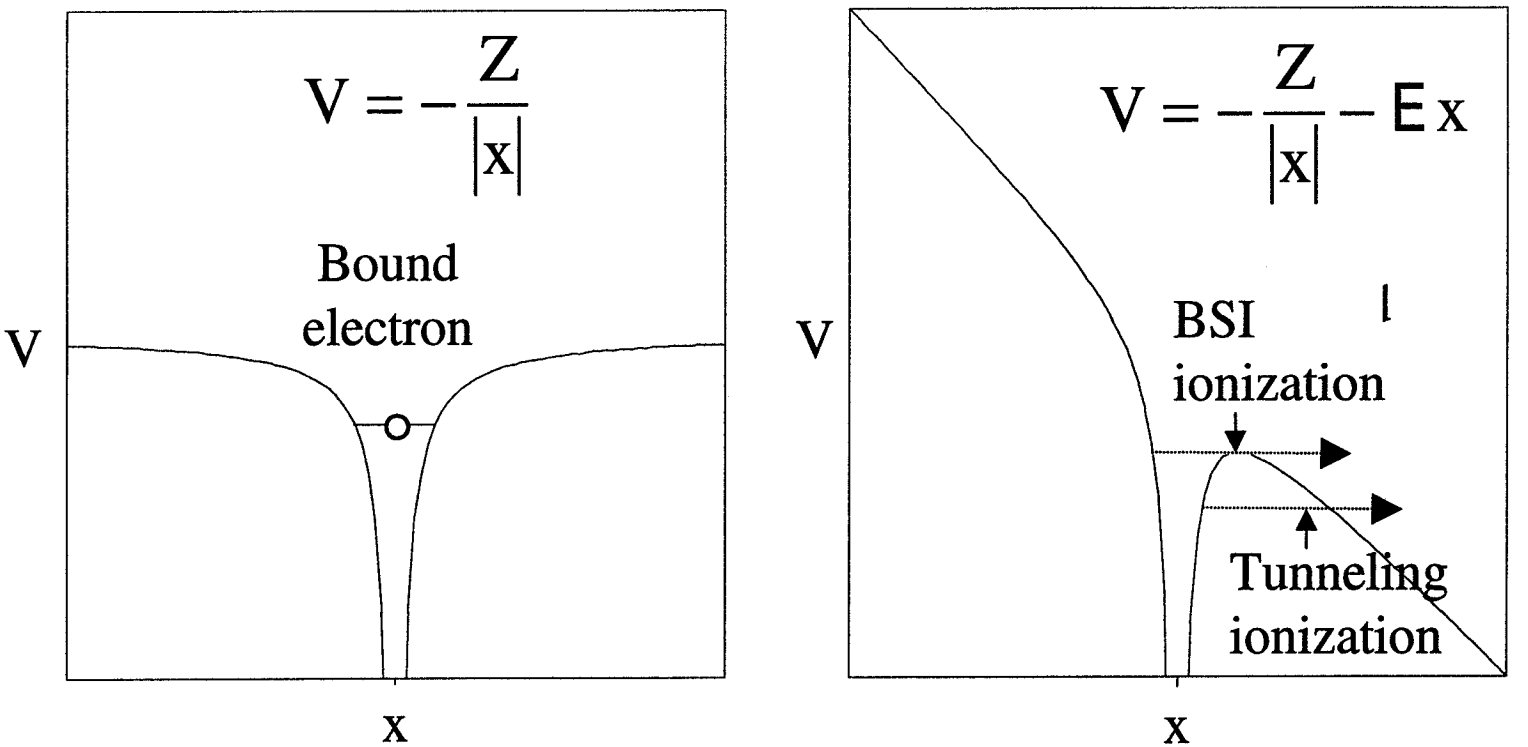

The critical electric field at which BSI ionization occurs is: $E_{crit} = \frac{E_{ion}^2}{4Z}$

An ionized electron is ejected from a laser focus by ponderomotive acceleration and conservation of canonical momentum

- An electron is accelerated from the laser focus by the gradient of the ponderomotive potential (average quiver energy)

$$\Phi_p = \frac{e^2\left\langle \vec{A}^2 \right\rangle}{2mc^2}$$

- An electron ionized with non-zero initial canonical momentum ($\vec{P}_0 = \vec{p}_0 + e\vec{A}_0/c$) has an average drift of:

$\vec{p}_d = \frac{e\vec{A}(\vec{r}_0, t_0)}{c}$, where $\vec{r}_0$ and t_0 are the position and time of ionization

- In circular polarization the direction of $\vec{p}_d$ does not have a fixed direction since $\vec{A}$ rotates in the plane of polarization. When considering many ionized electrons, there is no preferred direction for $\vec{p}_d$ resulting in cylindrically symmetric electron distributions
- In linear polarization $\vec{p}_d$ is always in the direction of polarization which causes an asymmetry in the electron distribution (peaked along $\vec{A}$ or $\vec{E}$).

Electrons ionized from higher charge states of ions produce higher energy electrons due to larger ponderomotive energies

Ion	I(W/cm^2)	Φ_p(keV)
Kr^{18+}	2.1×10^{18}	220
Kr^{17+}	1.7×10^{18}	180
Kr^{16+}	1.4×10^{18}	150
⋮	⋮	⋮

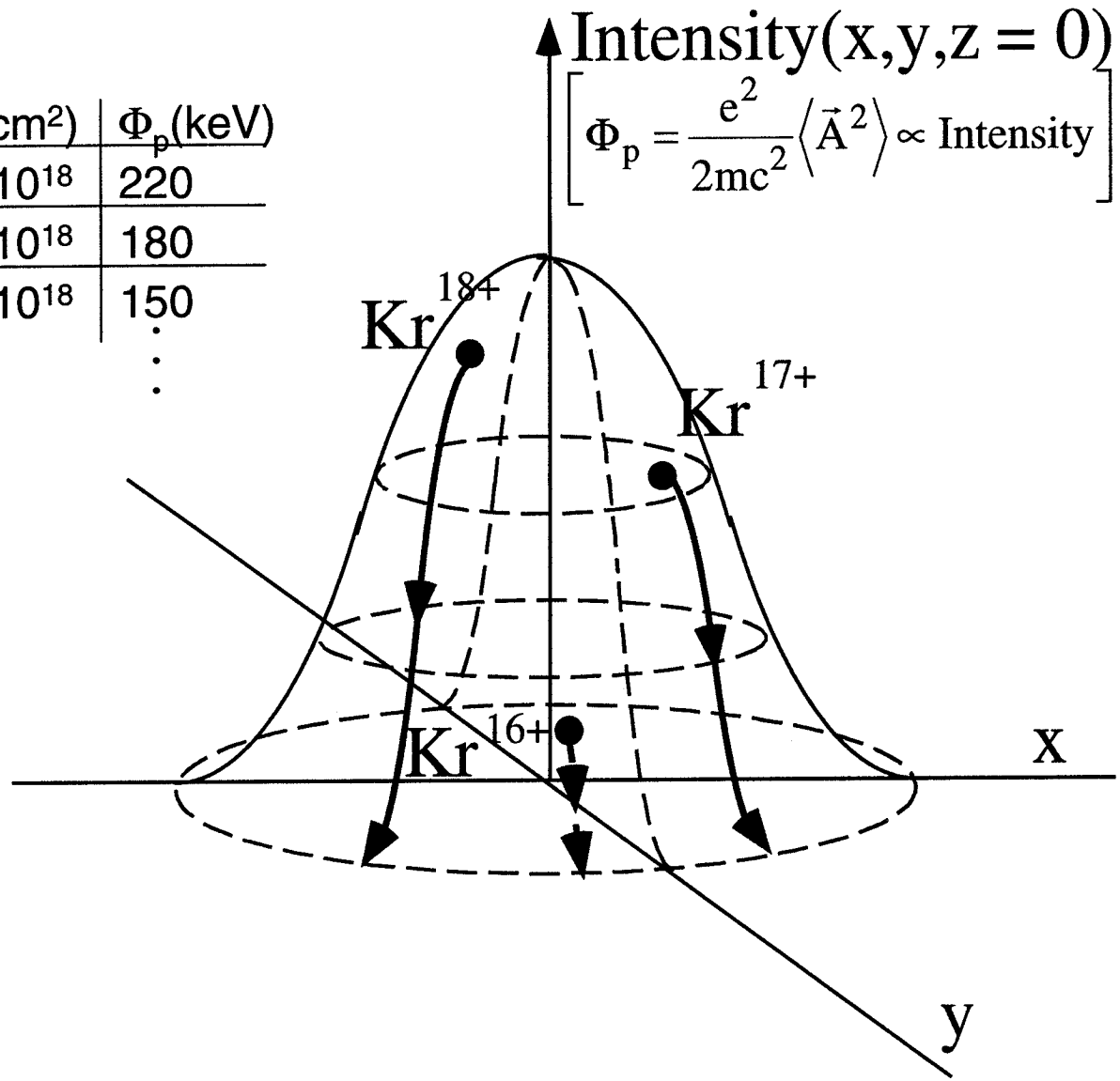

The ponderomotive force from a low intensity Gaussian laser focus is symmetric about the beam waist and predominantly radial:

The ponderomotive force of a diffraction limited Gaussian TEM_{00} focus is

$$\vec{F}_p = \vec{\nabla}\Phi_p \propto \left(\frac{w_0}{w(z)}\right)^2\left[\hat{r}\frac{2r}{w^2(z)} + \hat{z}\frac{z}{z_0^2}\left(\frac{w_0}{w(z)}\right)^2\left(1-2\left(\frac{r}{w(z)}\right)^2\right)\right]\mathrm{Exp}\left(-2\left(\frac{r}{w(z)}\right)^2\right)$$

where

$$w_0 = \frac{2\lambda f^{\#}}{\pi} \quad \text{and} \quad z_0 = \frac{4\lambda\left(f^{\#}\right)^2}{\pi}.$$

Three important features of this force are

$\vec{F}_p$ **is independent of** Φ, $F_z(z) = -F_z(-z)$, **and** $\frac{F_z}{F_r} \sim \frac{1}{4f^{\#}}\left(\sim\frac{1}{20}\right)$

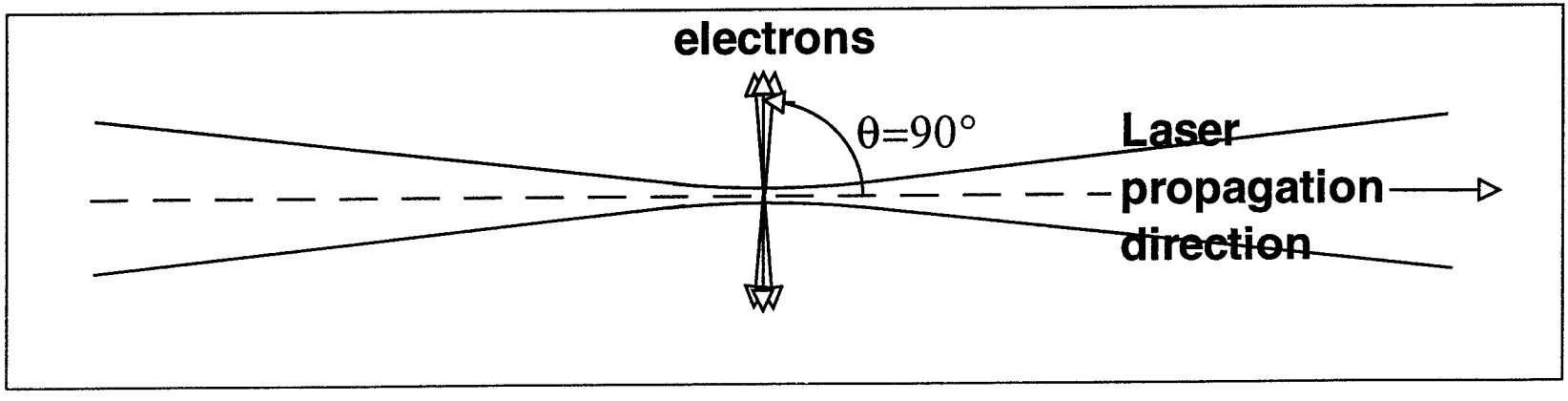

An electron interacting with high-field strengths gains momentum in the laser propagation direction

- **The low-intensity distribution of electrons ejected at 90º to the beam axis is "pushed" forward into a cone about the laser axis as the electron motion becomes relativistic**
- **This forward momentum component results from $\vec{v} \times \vec{B}$ or field momentum effects[1,2]**

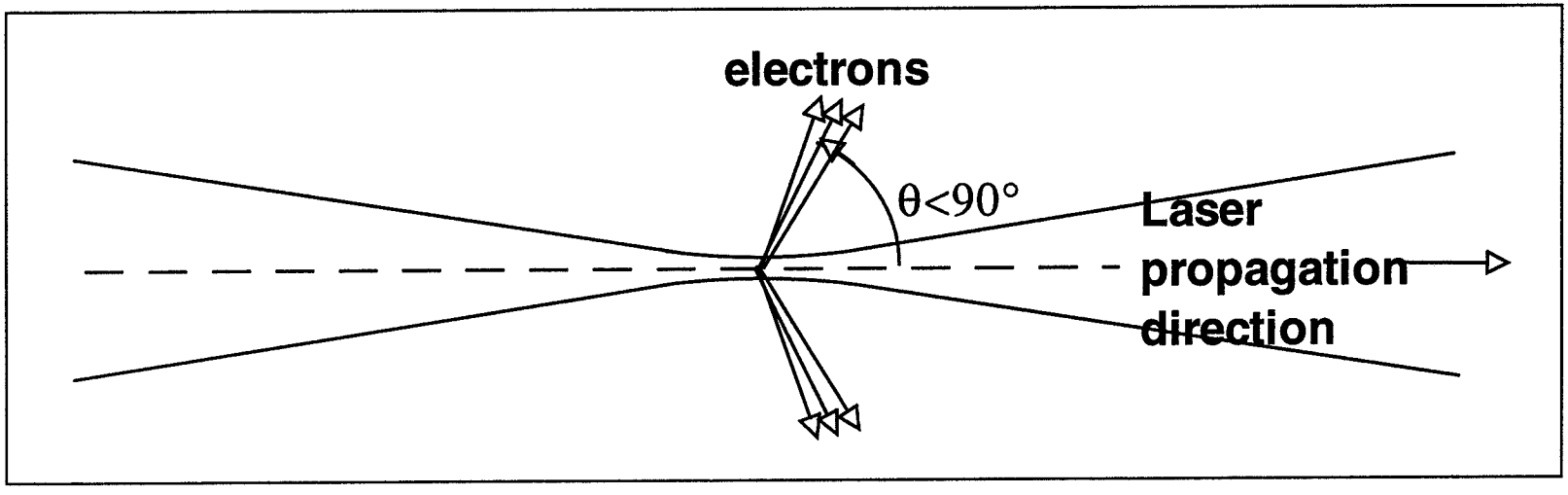

---

[1] C.I. Moore *et al.*, *Phys. Rev. Lett.* 74, 2439 (1995)

[2] H.R. Reiss, *J. Opt. Soc. Am. B* 7, 574 (1990); P.B. Corkum et al., in *Atoms in Intense Laser Fields*, edited by M. Gavrila (Academic, New York, 1992), p. 109; Y.I. Salamin and F.H.M. Faisal, *Phys. Rev. A* 55, 3678 (1997)

Derivation of energy-angle relation from Lorentz Force

$$\dot{\vec{p}} = -e\vec{E} - \frac{e}{\gamma mc}\vec{p}\times\vec{B} \approx -e\vec{E} - \frac{e}{\gamma mc}\vec{p}\times\left(\hat{k}\times\vec{E}\right) \quad [\text{assumes } \vec{B} = \hat{k}\times\vec{E}]$$

$$\dot{\vec{p}} = -e\vec{E} - \frac{e}{\gamma mc}\left(\vec{p}\cdot\vec{E}\right)\hat{k} + \frac{e}{\gamma mc}\left(\vec{p}\cdot\hat{k}\right)\vec{E} = -e\left(1 - \frac{e}{\gamma mc}\left(\vec{p}\cdot\hat{k}\right)\right)\vec{E} - \frac{e}{\gamma mc}\left(\vec{p}\cdot\vec{E}\right)\hat{k}$$

but $\vec{p}\cdot\frac{d\vec{p}}{dt} = -e\left(\vec{p}\cdot\vec{E}\right)$ and therefore:

$$\dot{\vec{p}} = -e\left(1 - \frac{e}{\gamma mc}\left(\vec{p}\cdot\hat{k}\right)\right)\vec{E} + \frac{1}{\gamma mc}\left(\vec{p}\cdot\frac{d\vec{p}}{dt}\right)\hat{k} = (\cdots) + \frac{1}{mc}\frac{1}{\sqrt{1+\vec{p}^2/m^2c^2}}\left(\vec{p}\cdot\frac{d\vec{p}}{dt}\right)\hat{k} \text{ or}$$

$$\dot{\vec{p}} = -e\left(1 - \frac{e}{\gamma mc}\left(\vec{p}\cdot\hat{k}\right)\right)\vec{E} + \frac{d}{dt}\sqrt{\vec{p}^2 + m^2c^2}\hat{k}$$

The z-component of this equation is:

$$\frac{dp_z}{dt} = \frac{d}{dt}\sqrt{\vec{p}^2 + m^2c^2} \quad \rightarrow \quad p_z(\vec{x},t) = \sqrt{\vec{p}^2(\vec{x},t) + m^2c^2} - \sqrt{\vec{p}^2(\vec{x},-\infty) + m^2c^2} + p_z(\vec{x},-\infty)$$

Assuming $\vec{p}(\vec{x},-\infty) = 0$ gives;

$$p_z(\vec{x},t) = \sqrt{\vec{p}^2(\vec{x},t) + m^2c^2} - mc.$$

Therefore:

$$\tan\theta = \frac{p_\perp}{p_z} = \frac{\sqrt{\vec{p}^2 - p_z^2}}{p_z} = \frac{\sqrt{\gamma^2 - 1 - (\gamma-1)^2}}{\gamma - 1} = \sqrt{\frac{2}{\gamma - 1}}.$$

Experiments and numerical simulations demonstrate the energy dependent ejection angle of LIPA

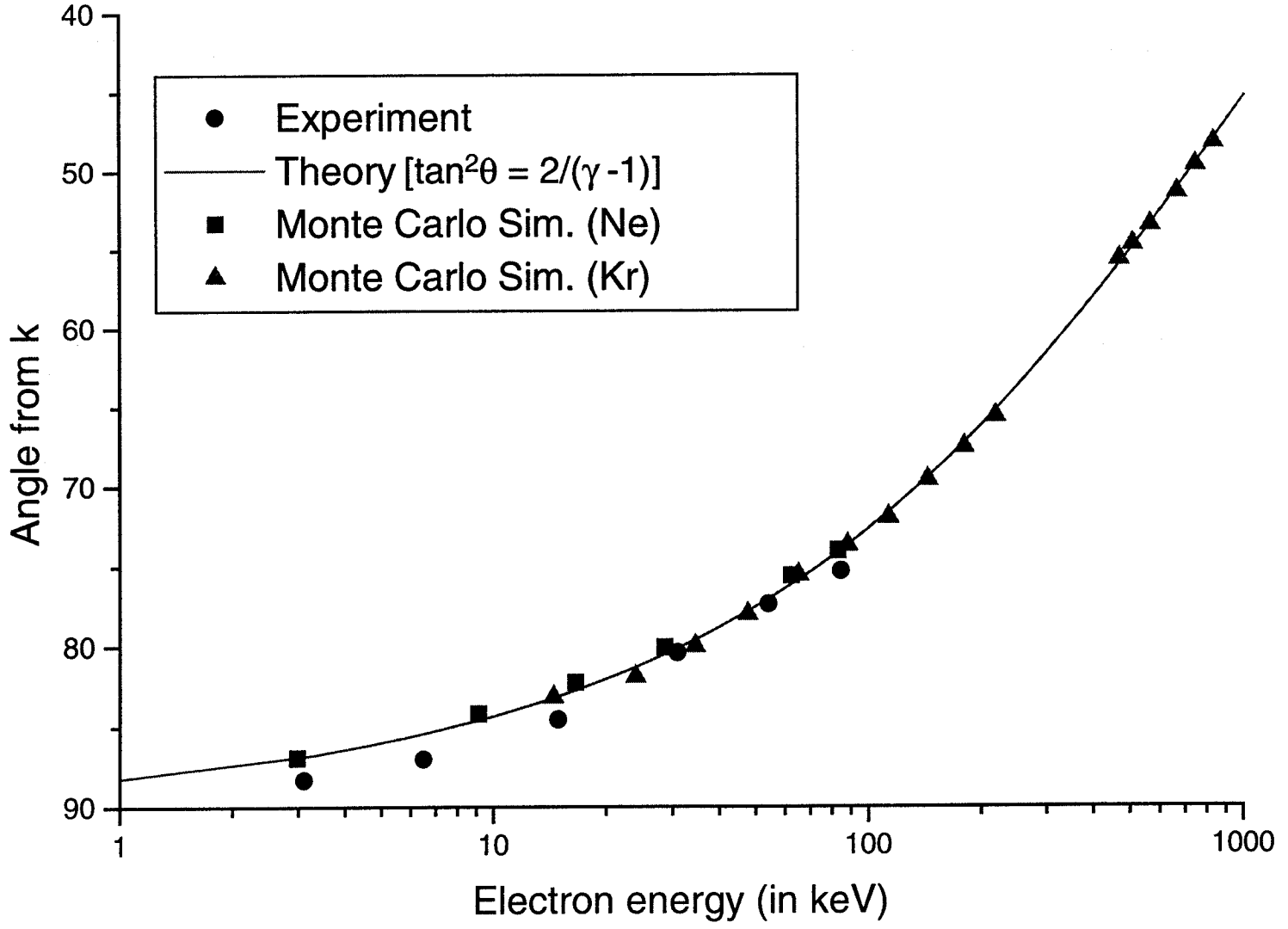

Ionized electrons are detected with DEF film bent into a cylinder and placed around the laser focus

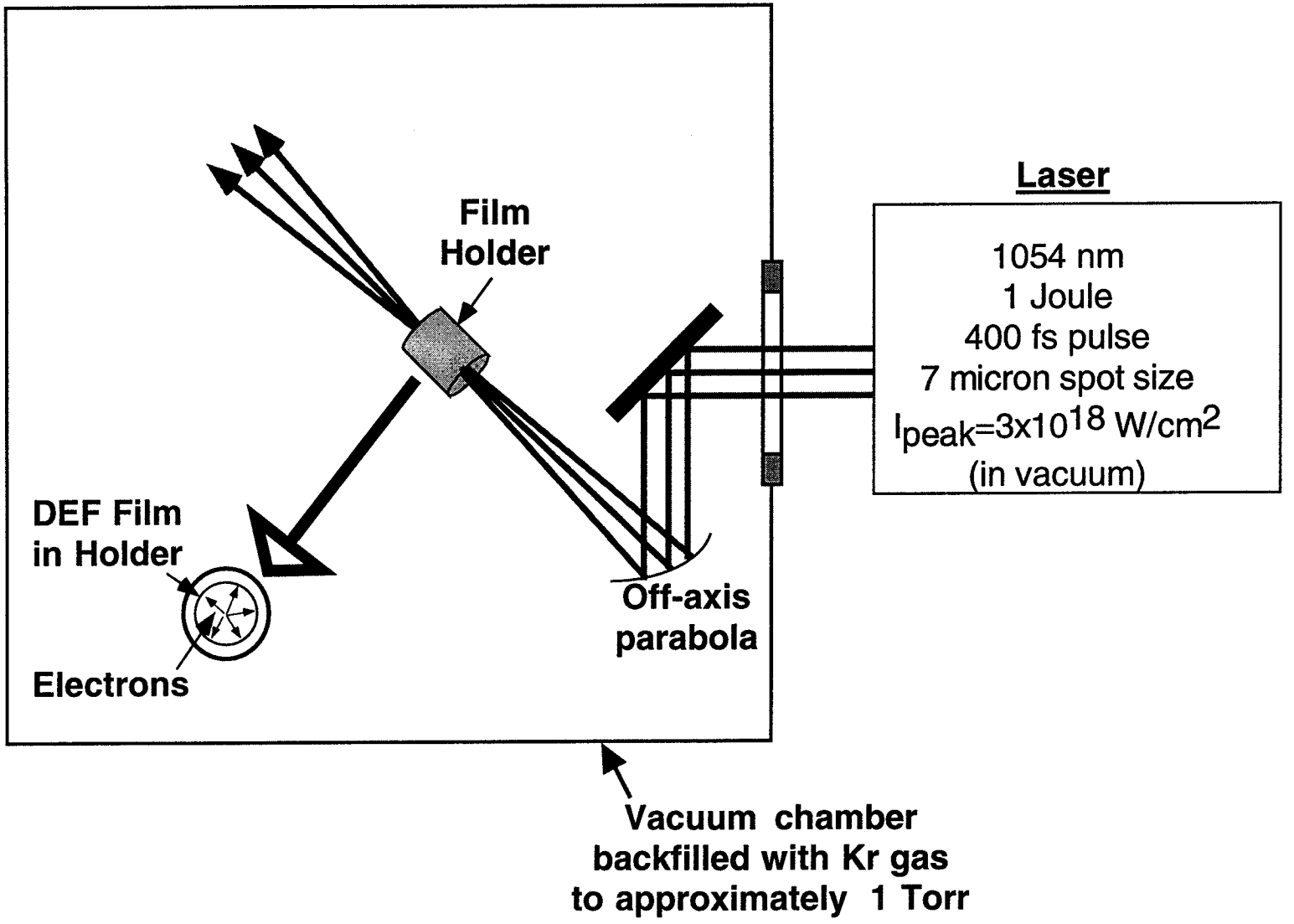

Ejected electron angular distribution from Krypton
(Circular polarization)

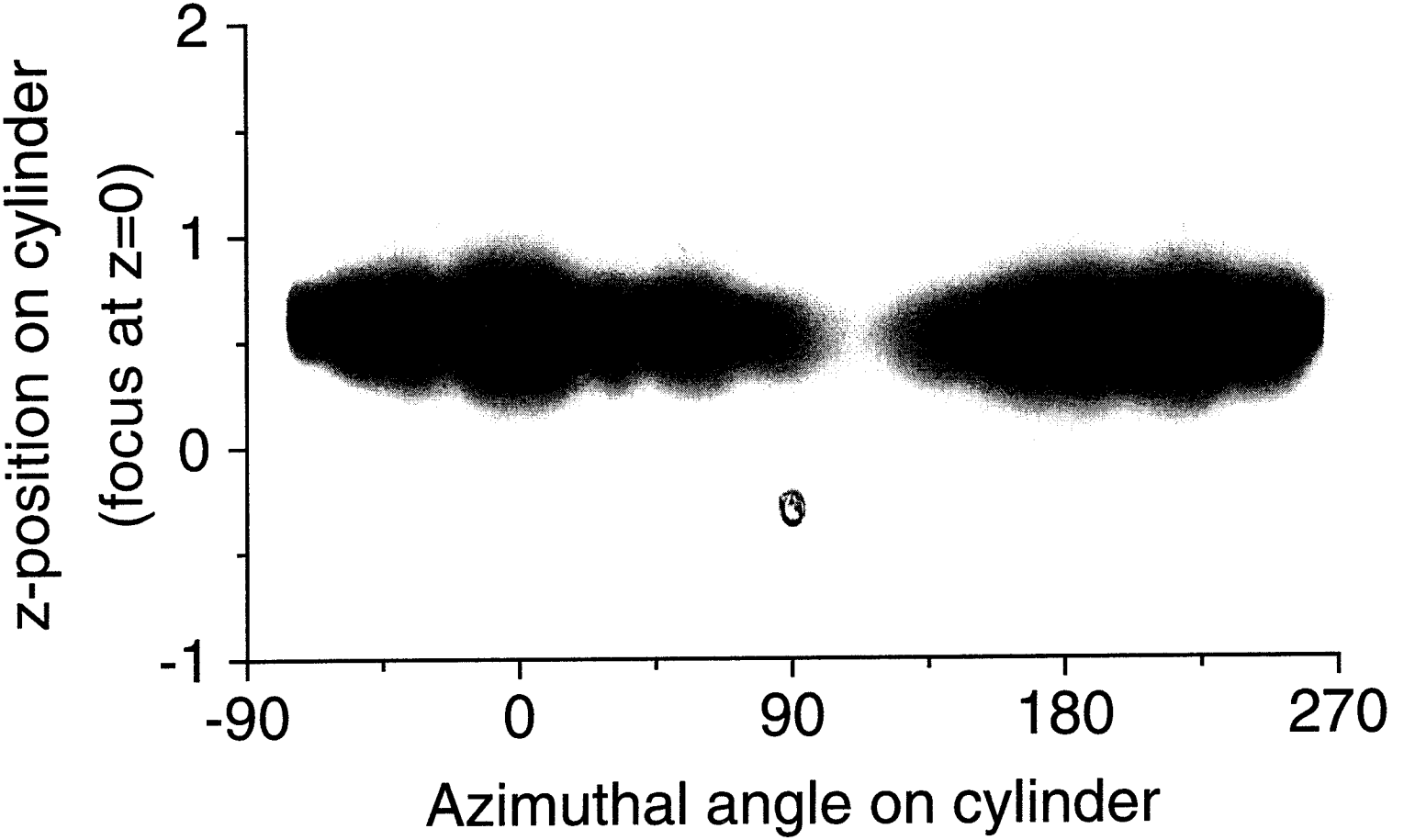

Ejected electron distributions from Krypton show electron ejection in the polarization direction (Φ=90° and Φ=270°) with a longitudinal momentum component (focus @ z=0)

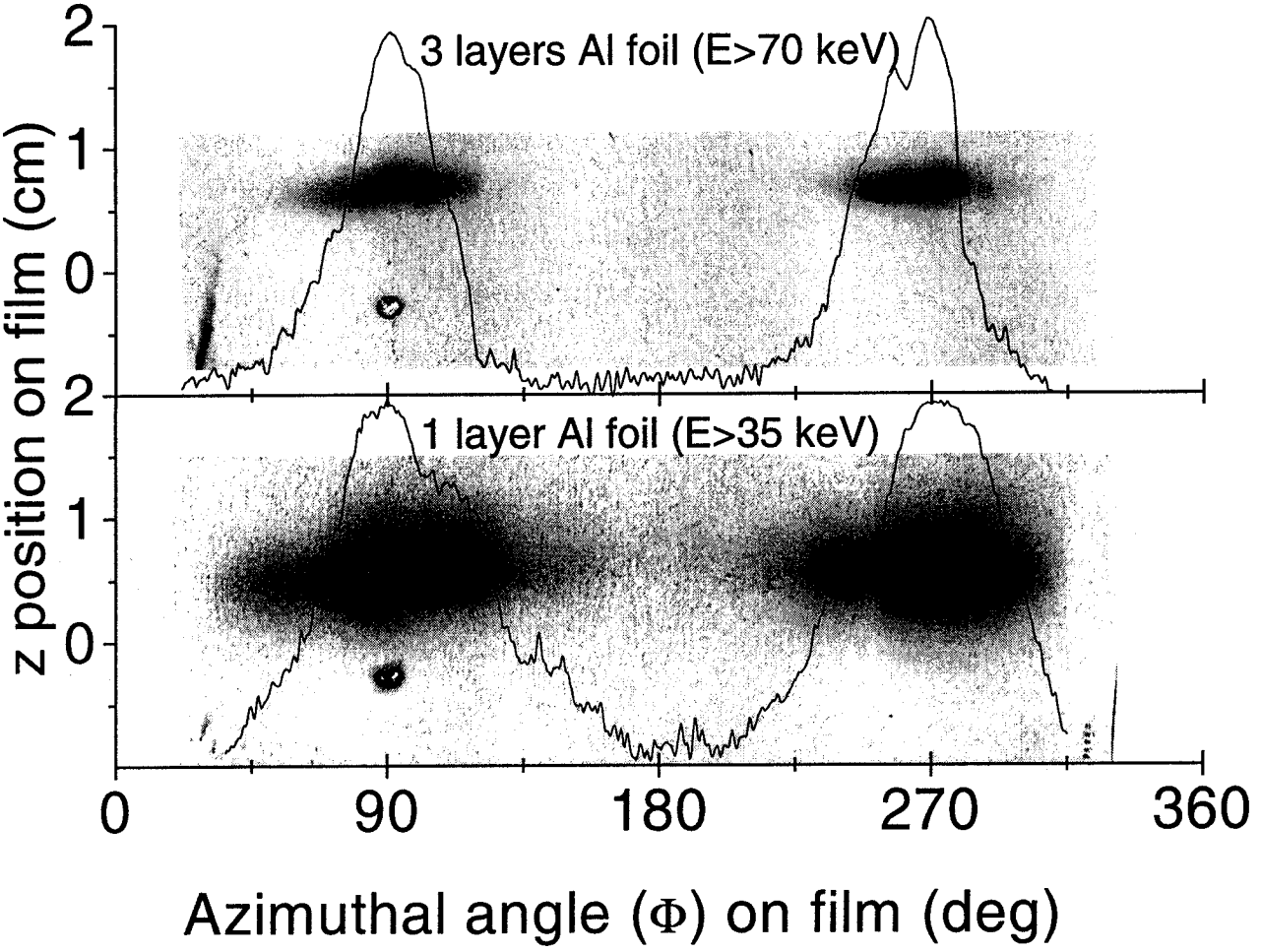

Observation of energy dependent ejection angle on film

- The electron angular distribution measured with 1 layer of aluminum foil over the film (E>35 keV) shows a maximum ejection cone angle of 80º (E≈32±20 keV).
- The distribution measured with 3 layers of aluminum foil (E>70 keV) shows a maximum ejection cone angle of 72º (E≈115±45 keV).
- The minimum ejection cone angle on both films is 59º (E≈360±90 keV).

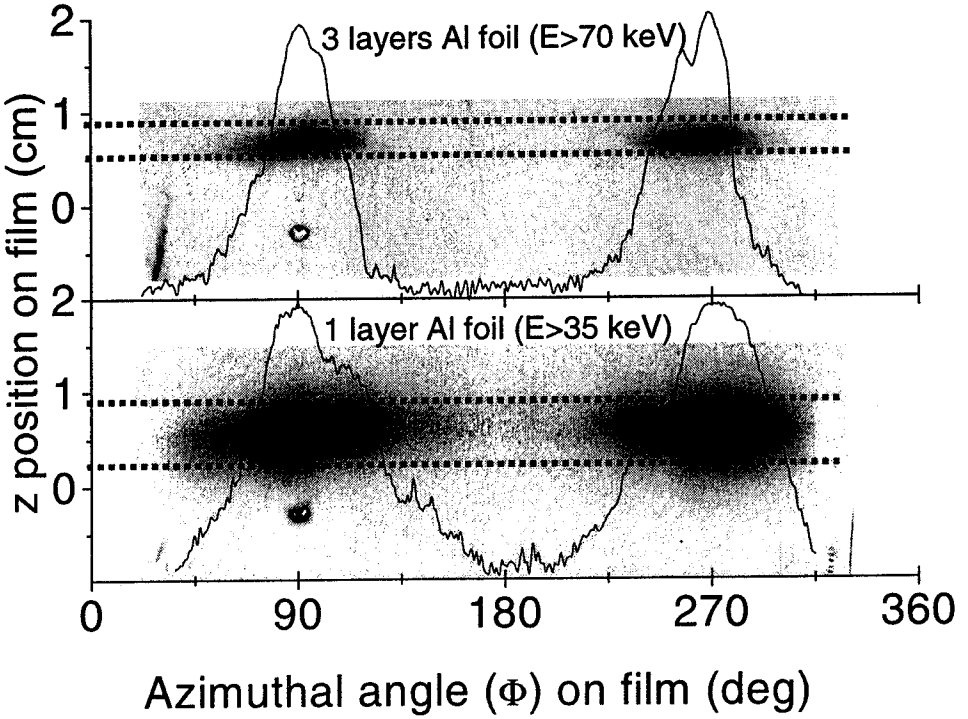

- **The relativistic equation of motion of each electron in the laser field is integrated to find the ejected electrons' trajectories,**

$$m\frac{dU^{\alpha}}{d\tau} = -\frac{e}{c}\left(\partial^{\alpha}A^{\beta} - \partial^{\beta}A^{\alpha}\right)U_{\beta} = -\frac{e}{c}E^{\alpha\beta}U_{\beta}.$$

A numerical simulation using Ammosov-Delone-Krainov (ADK) tunneling theory was used to model the experiment

- **Atoms are placed at random throughout the laser focus.**
- **A spatially and temporally Gaussian laser pulse is passed over the atoms in the laser focus.**
- **The field is modeled by the paraxial approximation for a Gaussian laser focus (including first order longitudinal field corrections).**
- **Ionization is modeled using ADK tunneling ionization rates[1]**
- **Following ionization, the relativistic equation of motion of each electron in the laser field is integrated to find the ejected electrons' trajectories,**

$$m\frac{dU^{\alpha}}{d\tau} = -\frac{e}{c}\left(\partial^{\alpha}A^{\beta} - \partial^{\beta}A^{\alpha}\right)U_{\beta} = -\frac{e}{c}E^{\alpha\beta}U_{\beta}.$$

---

[1] M.V. Ammosov *et al.*, *Sov. Phys. JETP* 64, 1191 (1986)

ADK tunneling ionization theory predicts much broader azimuthal electron distributions than observed in the experiment.

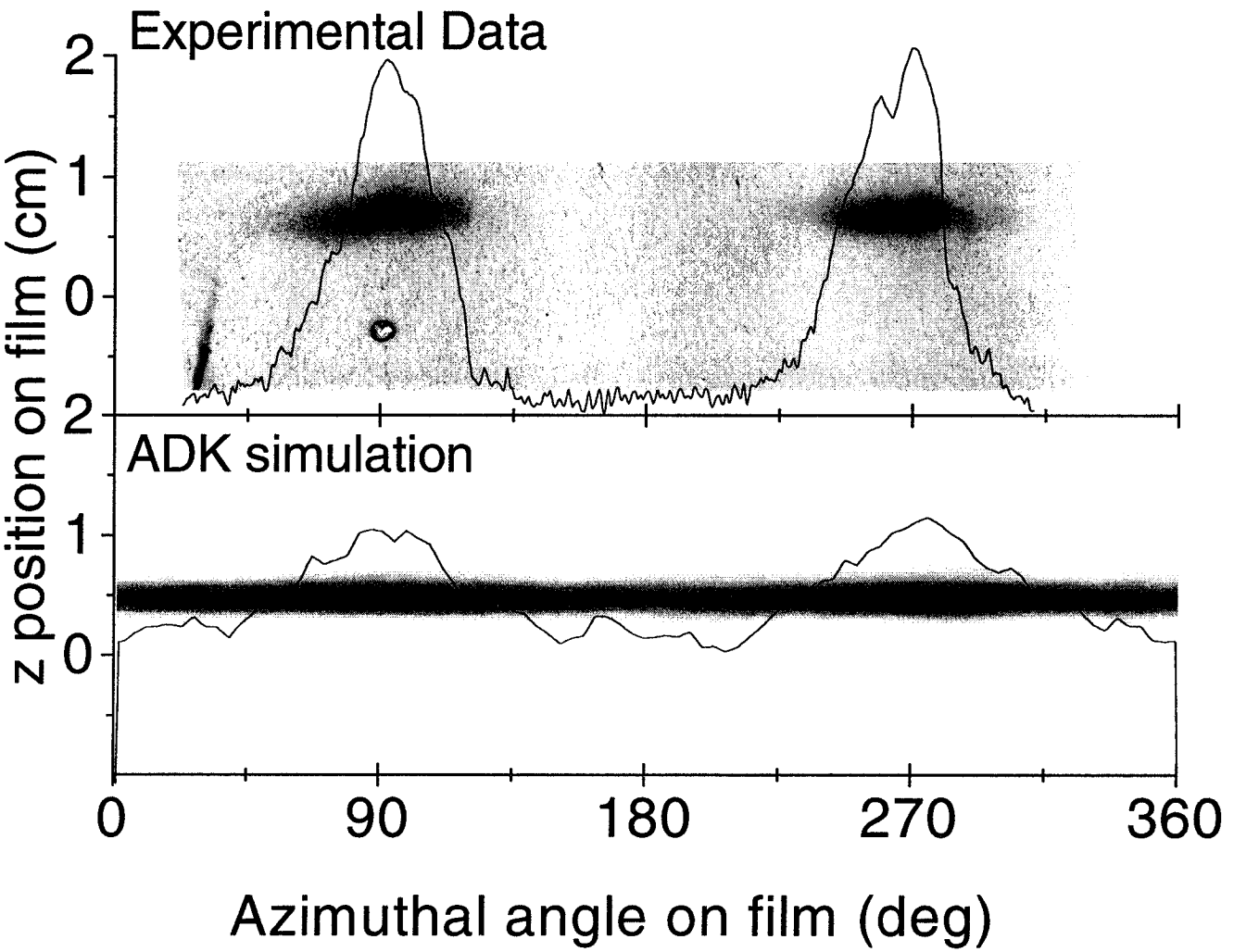

An ADK tunneling ionization simulation has been used to model the electron trajectories after ionization

- Atoms are placed at random throughout the laser focus.
- A spatially and temporally Gaussian laser pulse is passed over the atoms in the laser focus.
- The field is modeled by the paraxial approximation for a Gaussian laser focus (including first order longitudinal field corrections).
- The fraction of atoms ionized at phase η_0 in ADK theory is given by:

$$C(\eta_0)=1-\exp\left(-\int_{-\infty}^{\eta_0} w(\eta)d\eta\right),$$ where w(η) is the ADK rate:

$$w(\eta)=\sum_{m=-l}^{l} C^2_{n^*,l^*} f_{l^*,m} I_p \left[\frac{2}{|E(\eta)|}(2I_p)^{3/2}\right]^{2n^*-|m|-1} \exp\left[-\frac{2}{3|E(\eta)|}(2I_p)^{3/2}\right],$$

C_{n^*,l^*} and $f_{l^*,m}$ are constants ~1, I_p is the ionization potential, E(η) is the electric field, n* is the ground state principal effective quantum number ($n^*=Z/(2I_p)^{1/2}$), and l and m are the orbital and magnetic quantum numbers respectively.

- This fraction is solved for η_0 using a randomly generated $C(\eta_0)$ as the probability of ionization to find the time of ionization for each individual charge state of each ion.

A second simulation using an empirical modification to BSI ionization theory was used to better model the experiment

- **The modified BSI simulation is identical to the ADK simulation except a different ionization model is used.**
- **The polarization directed electrons observed in the experiment suggest electrons are ionized with larger initial canonical momentum ($\vec{P}_0 = \vec{p}_0 + e\vec{A}_0/c = e\vec{A}_0/c$) than predicted by ADK theory.**
- **To produce this large initial canonical momentum, BSI theory was modified to simulate ionization at a wider range of phases than predicted by ADK:**

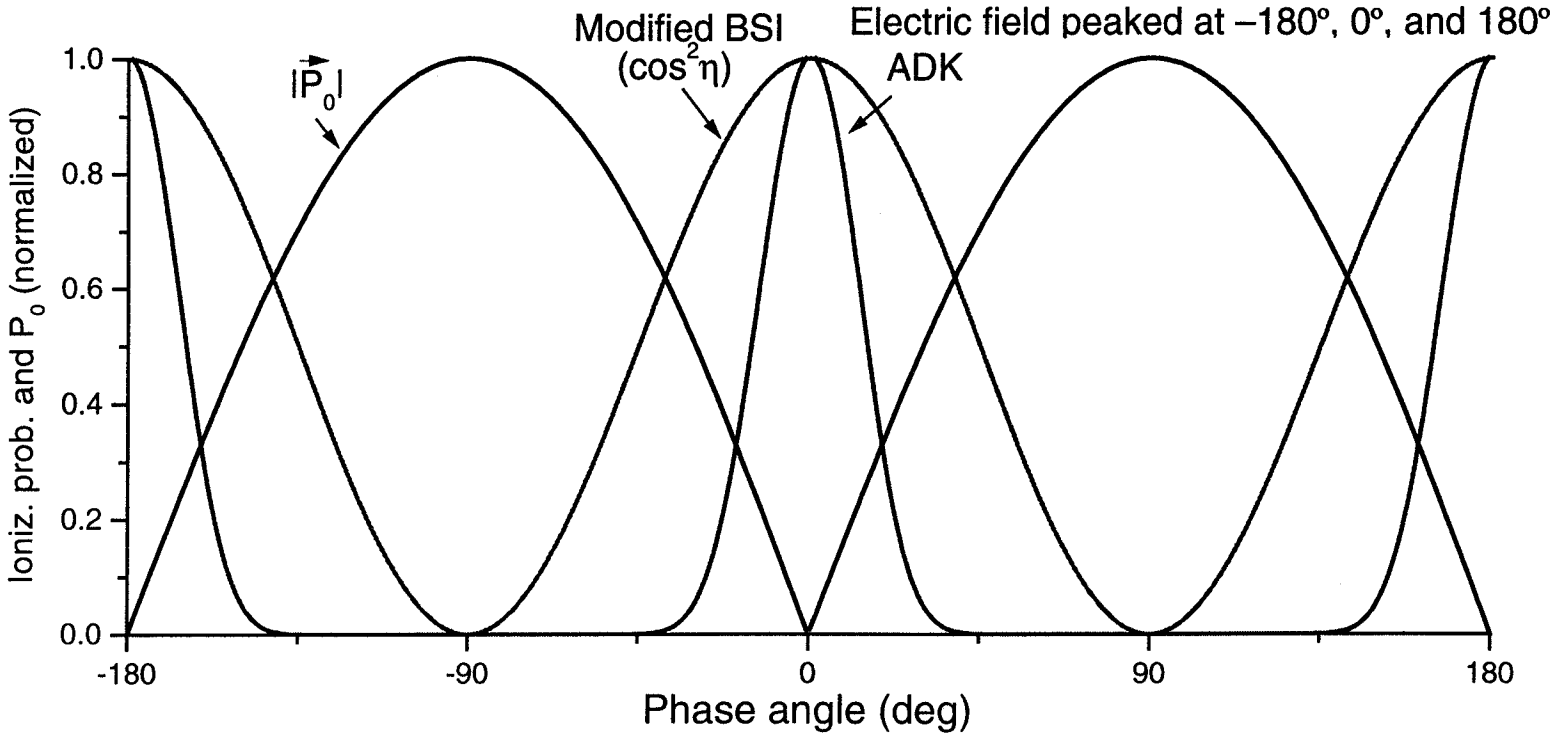

Ionization with larger P_{can} than predicted by ADK tunneling theory shows electron angular distributions consistent with the experimental results

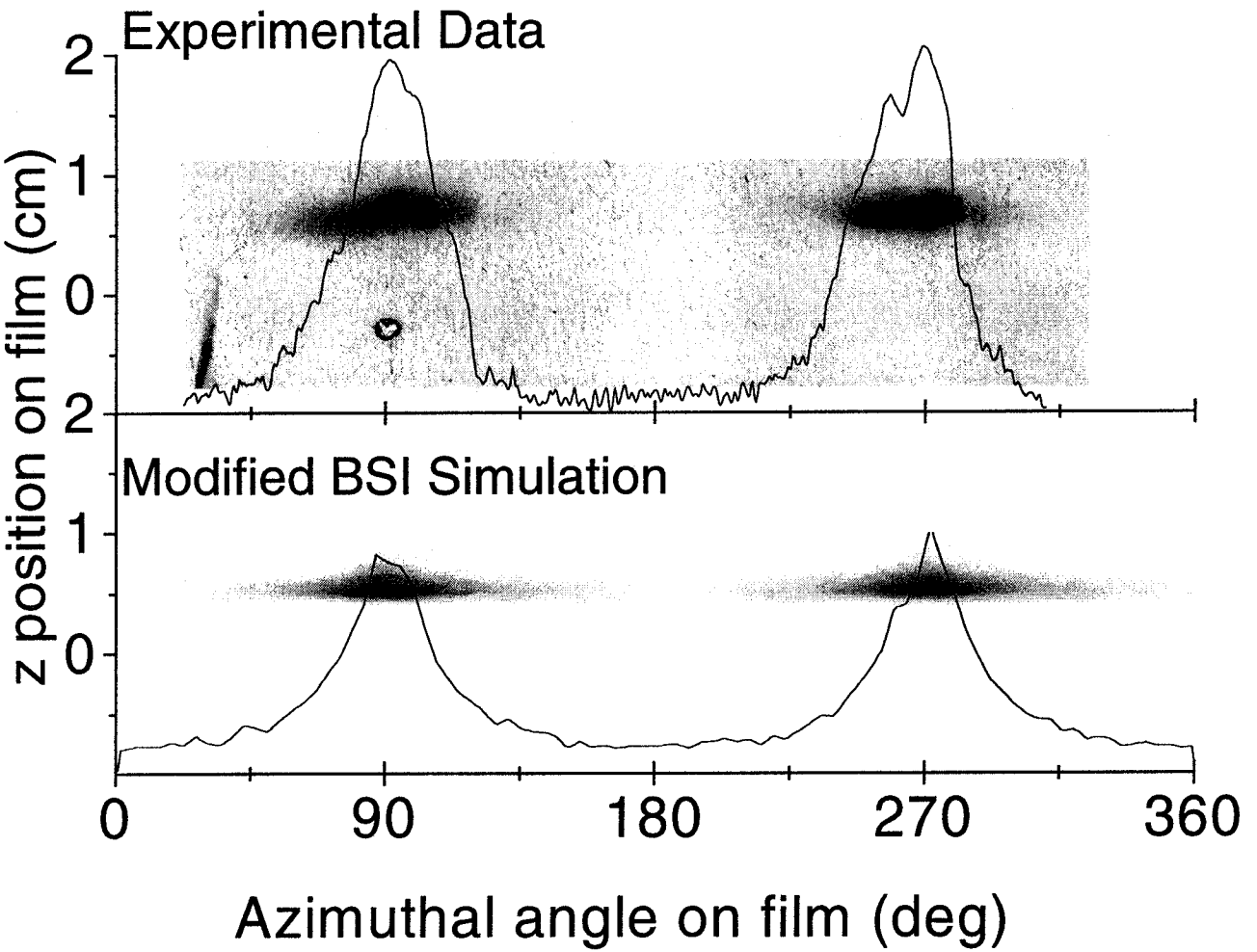

Experimental setup for electron energy spectrum measurements

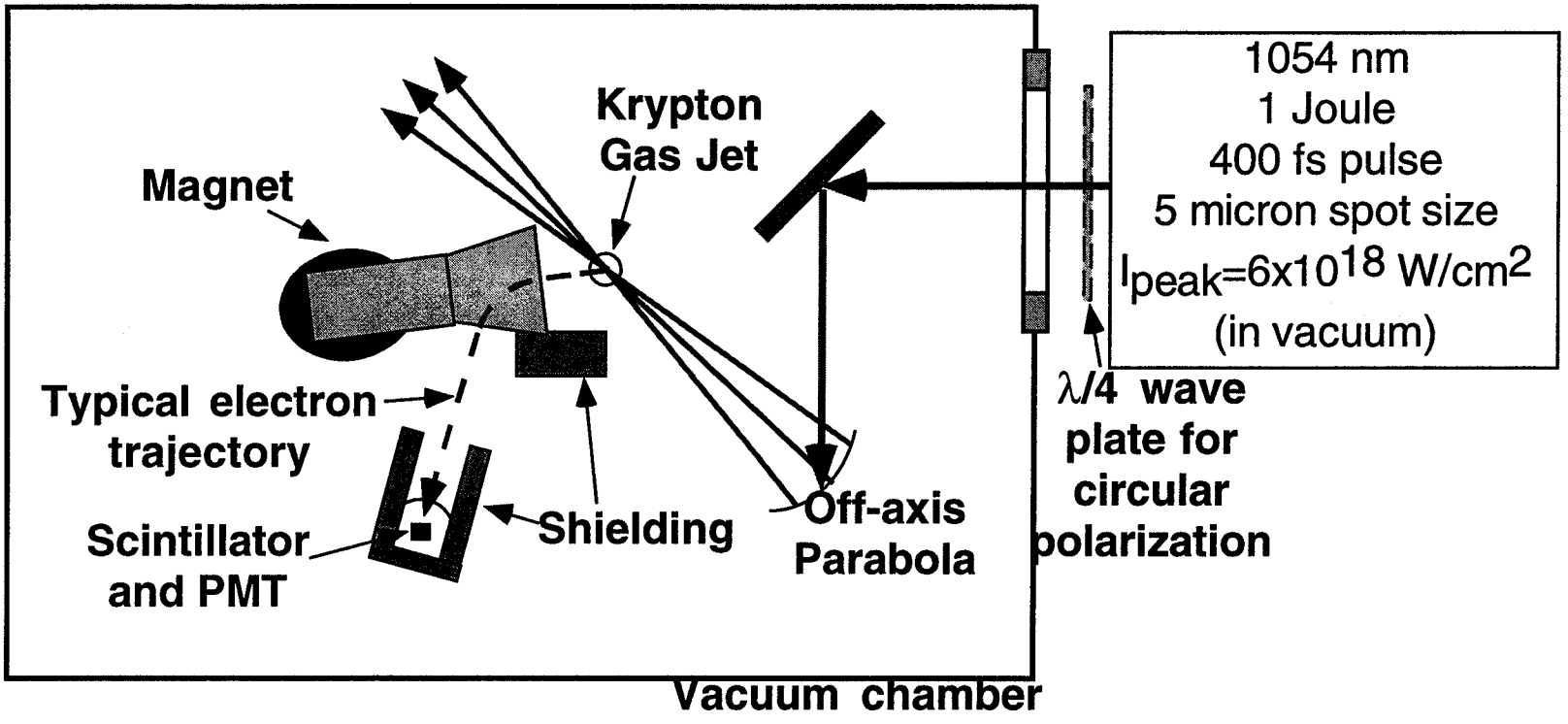

LIPA electron energy spectrum in linear and circular polarization

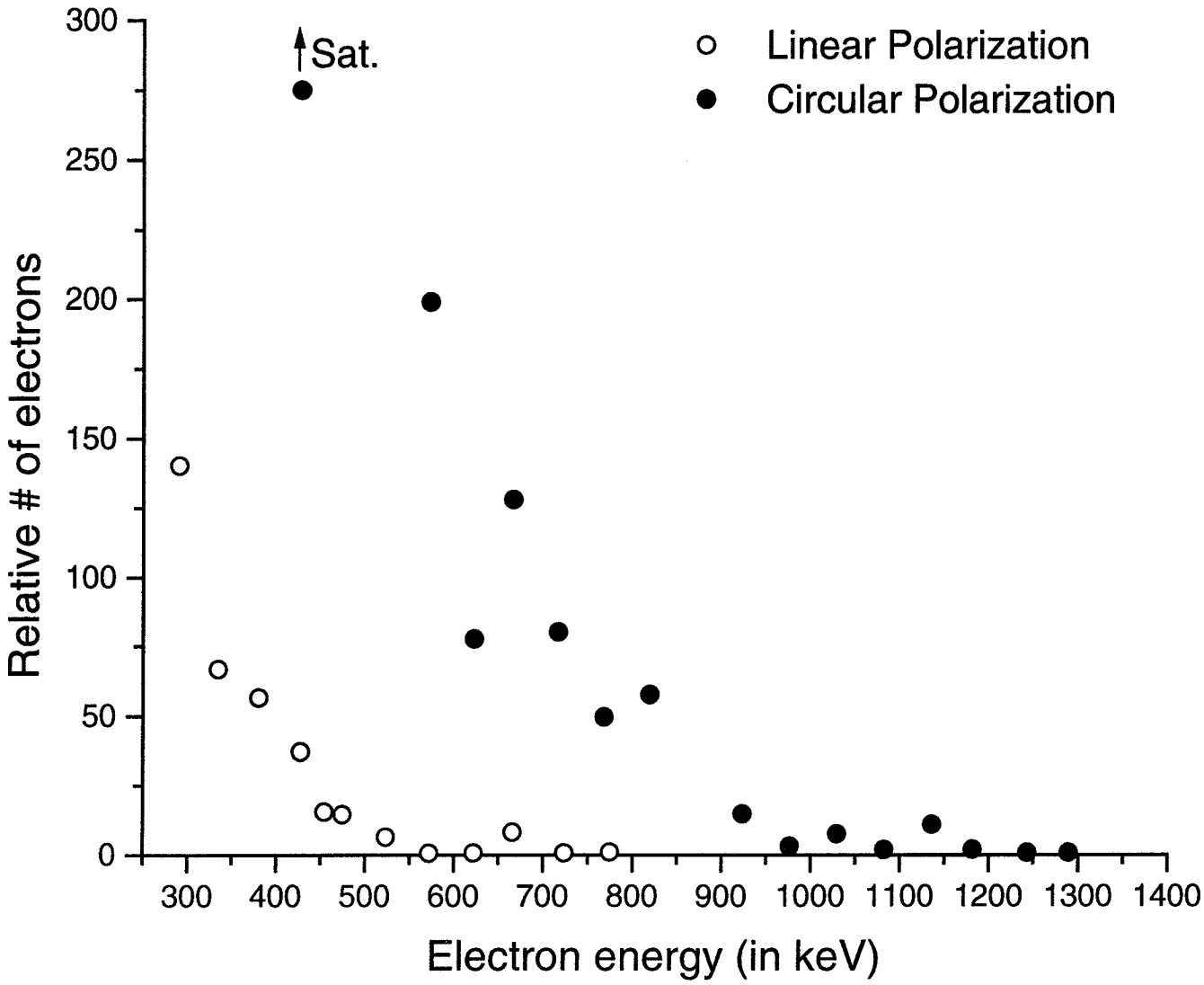

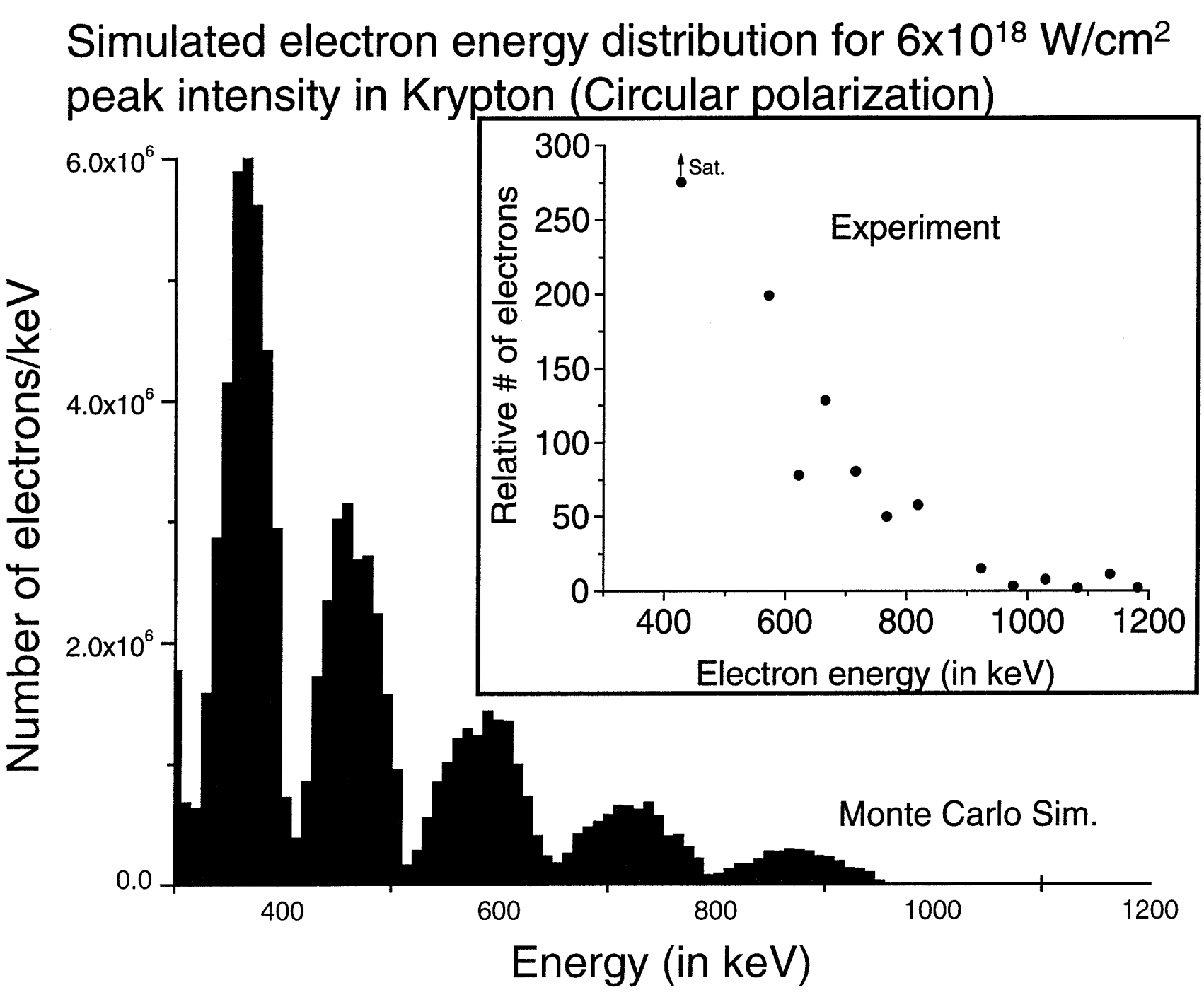
Simulated electron energy distribution for 6x10^18 W/cm^2 peak intensity in Krypton (Circular polarization)
Number of electrons/keV
6.0x10^6
4.0x10^6
2.0x10^6
0.0
400
600
800
1000
1200
Energy (in keV)
Monte Carlo Sim.
Relative # of electrons
300
250
200
150
100
50
0
Sat.
Experiment
400
600
800
1000
1200
Electron energy (in keV)

Ejected electron energy distribution for 6×10^{18} W/cm^2 peak intensity in Krypton (Linear polarization)

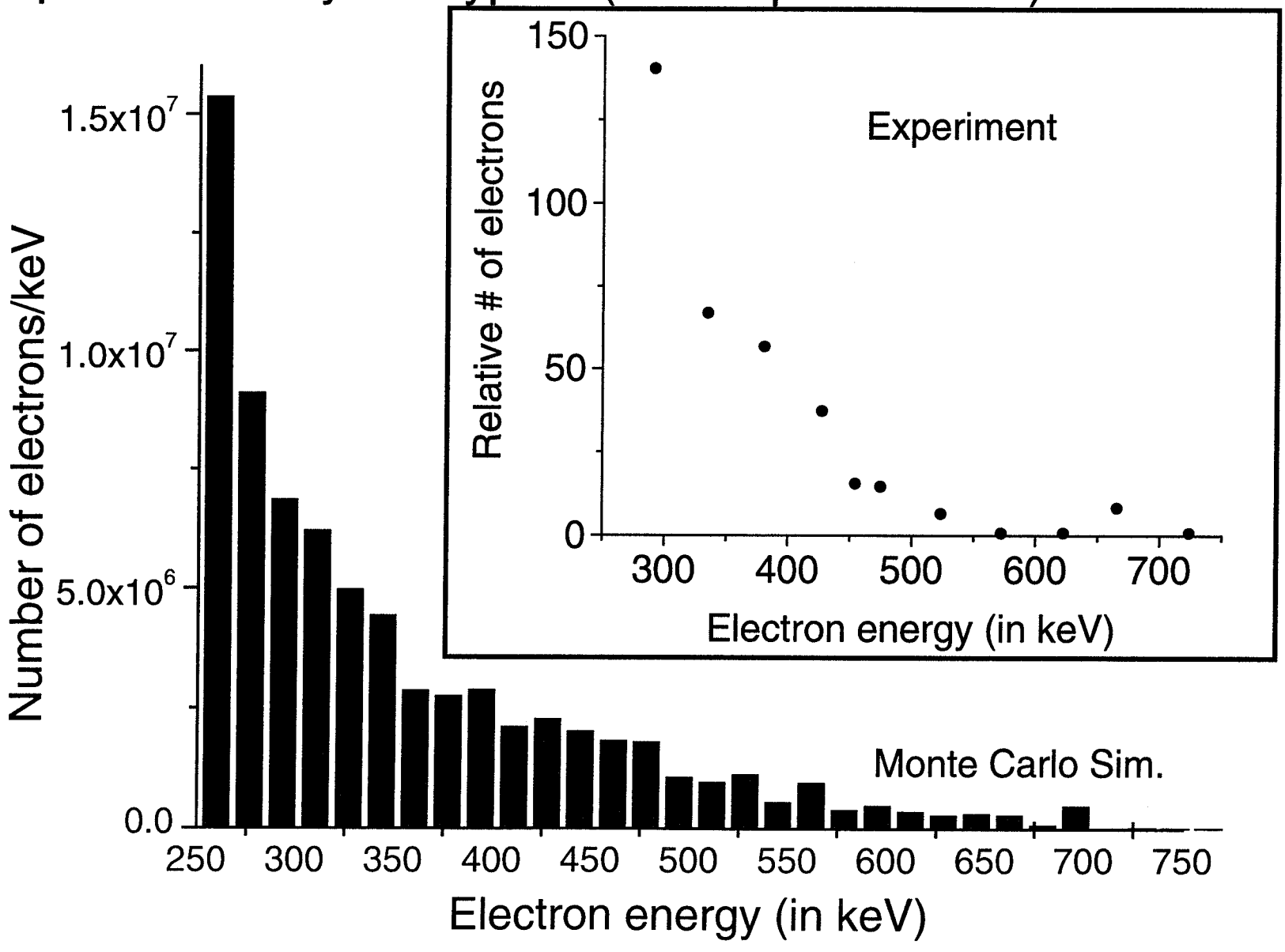

Simulations of high intensity ionization (I_{peak}=2x10^{19} W/cm^2) of Argon using 7.5 TW from upgraded T^3 laser pulse

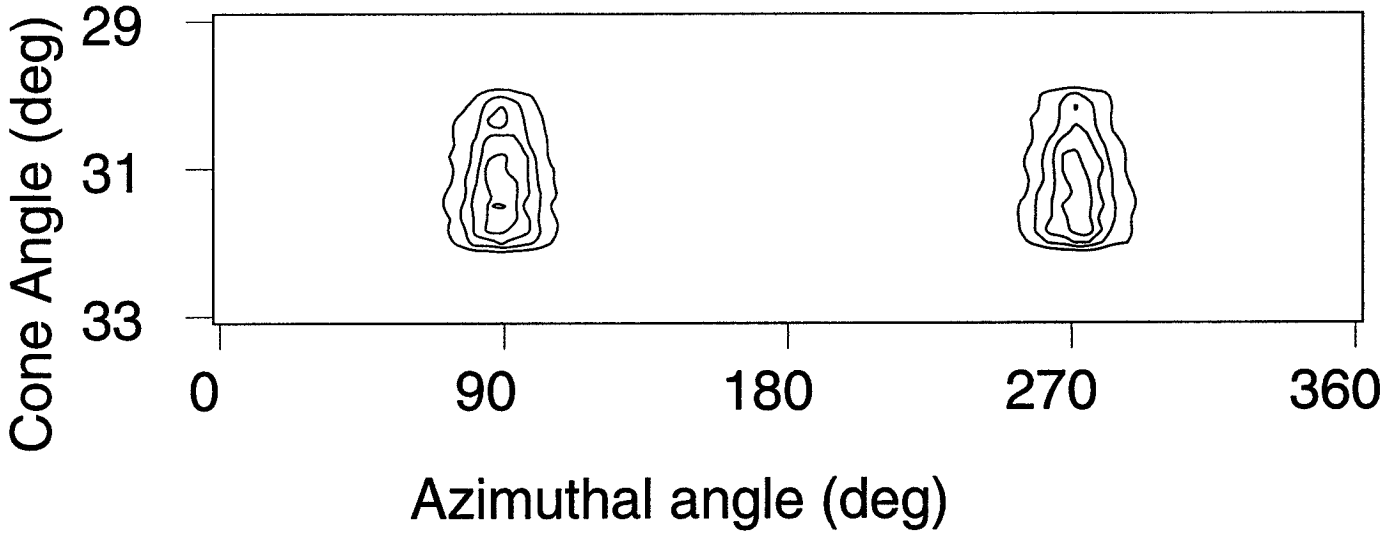

Each ejected electron beam has the following characteristics:

- Energy = 2.8 MeV with an energy spread of 300 keV FWHM
- $\varepsilon \approx 0.8$ mm-mrad
- $q \approx 2$ pC
- Electron pulse length $\approx$ 100 fs

Experimental setup using LIPA electrons as the injector for a laser based accelerator.

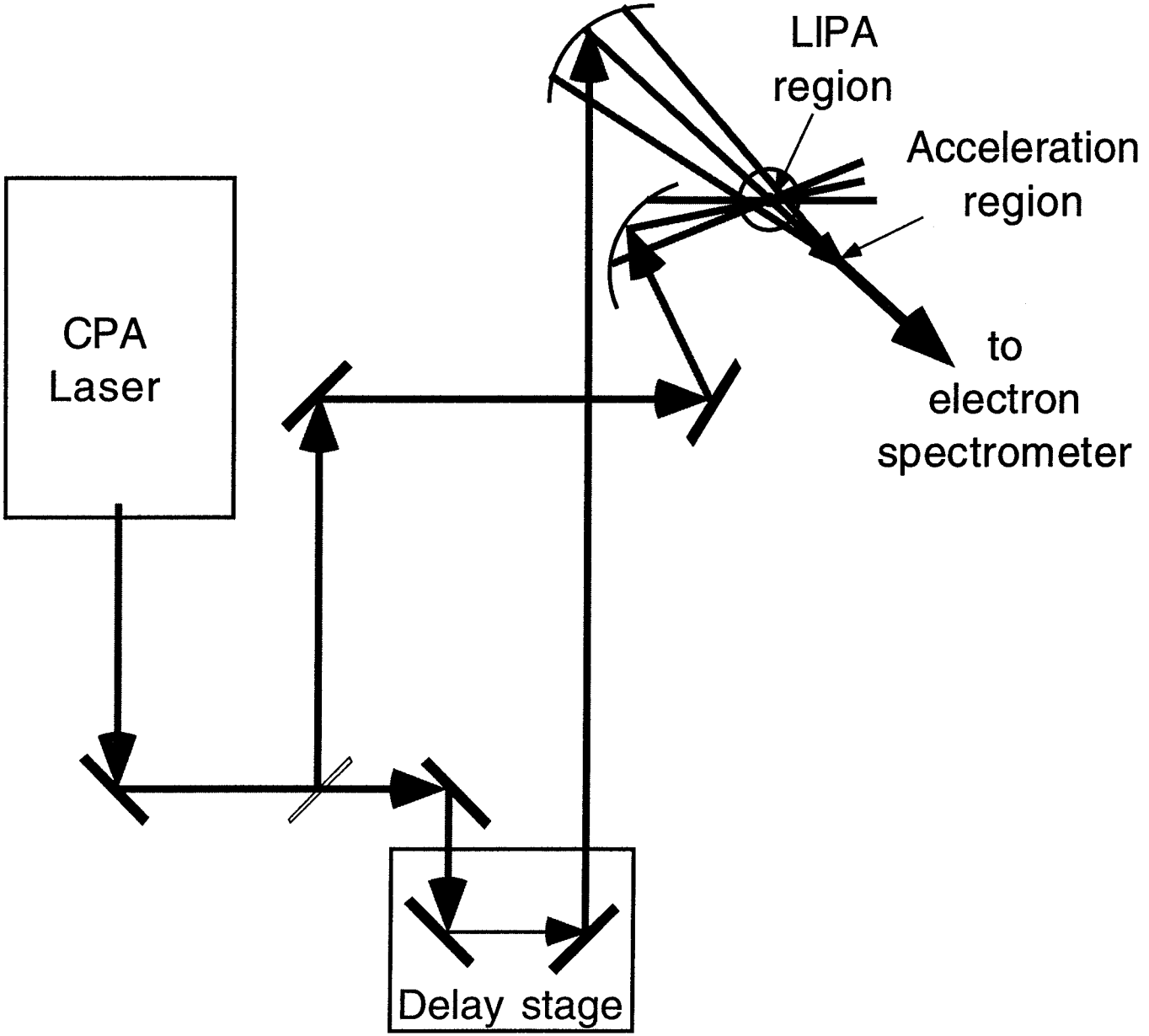

Electron energy spectrum of Argon using $I_{peak}=5x10^{22}$ W/cm^2

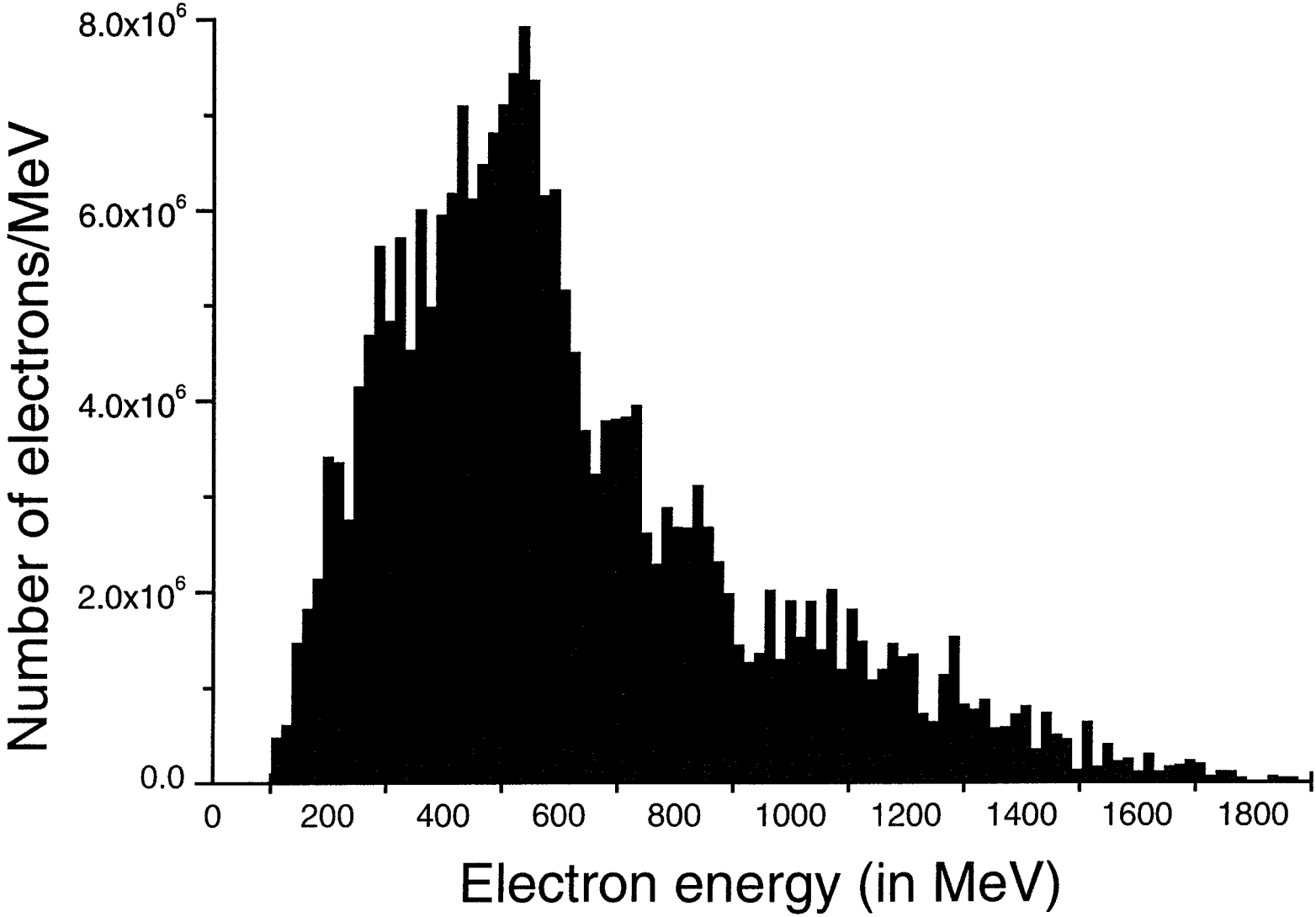

Conclusions

- Ultrashort pulse electron bunches can be produced for injection into laser driven accelerators such as the LWFA.
- Experiments on LIPA electron injector demonstrated:

  —using a linearly polarized laser pulse, two highly directional electron beams ($\Omega \approx 0.05$ SR) in the laser polarization direction with energies up to approximately 500 keV.

  —using a circularly polarized laser pulse, production of a roughly annular electron beam with energies up to 1 MeV.
- Numerical simulations on LIPA show:

  —using the well accepted ADK tunneling ionization theory, electron distributions inconsistent with the experimental observations.

  —Using a simulation imposing larger initial canonical momentum than predicted by ADK theory, much better agreement with the observations.
- Simulations show excellent emittance short pulse electron beams are produced using LIPA.
- Petawatt lasers capable of achieving near diffraction limited focal quality could produce up to 1 GeV electrons using the LIPA mechanism.